Transport and Aggregation of Self-Propelled Particles in Fluid Flows

Colin Torney and Zoltán Neufeld

School of Mathematical Sciences and Complex and Adaptive Systems Laboratory, University College Dublin, Belfield, Dublin 4, Ireland

(Received 12 April 2007; published 13 August 2007)

An analysis of the dynamics of prolate swimming particles in laminar flow is presented. It is shown that the particles concentrate around flow regions with chaotic trajectories. When the swimming velocity is larger than a threshold, dependent on the aspect ratio of the particles, all particles escape from regular elliptic regions. For thin rodlike particles the threshold velocity vanishes; thus, the arbitrarily small swimming velocity destroys all transport boundaries. We derive an expression for the minimum swimming velocity required for escape based on a circularly symmetric flow approximation of the regular elliptic regions.

DOI: 10.1103/PhysRevLett.99.078101 PACS numbers: 87.18.Ed, 05.45.−a, 45.70.Qj

The study of transport, mixing, and pattern formation within suspensions of swimming microorganisms has many applications for biotechnology, oceanic ecology, and evolutionary biology. Dynamical systems methods applied to the transport of passive tracers have given some insight into the role of chaotic trajectories and impenetrable transport barriers for mixing in laminar flows, while experiments with motile microorganisms and theoretical models of self-propelled particles have demonstrated a rich variety of self-organization phenomena including bioconvection, generation of coherent jets and vortices, collective motion, etc. [1–4]. In these examples the coherent behavior results from oriented swimming in response to external fields like chemical concentration (chemotaxis), illumination, gravitational torque, or is created via direct or indirect interactions between the particles. In this Letter we analyze the effect of swimming on the transport properties of steady and unsteady laminar flows and examine the spatial distribution of self-propelled particles when their shape and swimming speed are varied.

We consider a dilute suspension of noninteracting prolate spheroid particles propelled along their principal axis and advected by an externally imposed flow. The magnitude of the swimming velocity v_p is assumed to be constant and typically small compared to the characteristic flow velocity. The swimming direction is determined by the particle orientation, represented by the unit vector $\mathbf{p}$. The motion of a particle is then described by

$$\dot{\mathbf{r}} = \mathbf{v}_f(\mathbf{r}, t) + v_p\mathbf{p}, \tag{1}$$

where $\mathbf{v}_f$ represents the velocity field of the ambient fluid.

The orientation of spheroidal particles in a fluid is governed by the local flow field according to [5]

$$\dot{\mathbf{p}} = \tfrac{1}{2}\boldsymbol{\omega} \times \mathbf{p} + \alpha\mathbf{p} \cdot \mathbf{E} \cdot (\mathbf{I} - \mathbf{pp}), \tag{2}$$

where $\boldsymbol{\omega} = \nabla \times \mathbf{v}_f$ is the vorticity, $\mathbf{E} = (\nabla\mathbf{v}_f + \nabla\mathbf{v}_f^T)/2$ is the rate of strain tensor, $\mathbf{I}$ is the identity matrix, and α is a parameter representing the particle eccentricity, defined as $\alpha = (\gamma^2 - 1)/(\gamma^2 + 1)$, where γ is the ratio of the major and minor axis of the spheroid.

We examine the dynamics of self-propelled particles in steady and unsteady two-dimensional laminar flows. Transport of passive particles in such flows is well understood. In the time-independent case passive particles simply follow the streamlines, while in unsteady flows the flow field is composed of well mixed regions filled with chaotic trajectories and islands of regular elliptic regions where particles move on quasiperiodic orbits that form impenetrable transport barriers (KAM tori) [6].

In the numerical simulations we model the velocity field by a cellular flow which exhibits the characteristic transport properties described above and has been studied both experimentally and theoretically for the mixing of passive tracers [7,8]. The velocity field of the cellular flow is defined by a stream function ψ as

$$\psi(x, y, t) = \frac{U_0 L}{2\pi} \sin\left(\frac{2\pi(x - x_0(t))}{L}\right) \sin\left(\frac{2\pi y}{L}\right), \tag{3}$$

where U_0 is the maximum velocity of the flow and L is the wavelength of the vortex chain. When x_0 is constant the flow is time independent and passive particles move periodically on closed streamlines within a cell. These cells are separated by separatrices that connect the saddle points $x = x_0 + nL/2$, $y = nL/2$, with n integer. For the time-dependent flow we introduce a lateral oscillation of the type used by Solomon and Gollub [8], $x_0(t) = B\sin(\omega t)$. This perturbation induces chaotic mixing of passive tracers in a region around the separatrices whose width increases with B, that leads to fast dispersion and large scale transport. Other particles move on regular quasiperiodic trajectories typically localized within a single cell (see the Poincaré section in Fig. 3).

In two dimensions the orientation of the self-propelled particles can be represented by an angle θ in the x-y plane, and (1) and (2) reduces to

$$\dot{\theta} = \alpha\left[\frac{1}{2}\left(\frac{\partial^2\psi}{\partial y^2} - \frac{\partial^2\psi}{\partial x^2}\right)\cos 2\theta - \frac{\partial^2\psi}{\partial x \partial y}\sin 2\theta\right] - \frac{1}{2}\left(\frac{\partial^2\psi}{\partial x^2} + \frac{\partial^2\psi}{\partial y^2}\right), \quad (4)$$

$$\dot{x} = \frac{\partial\psi}{\partial y} + v_s\cos\theta, \qquad \dot{y} = -\frac{\partial\psi}{\partial x} + v_s\sin\theta.$$

We nondimensionalize the equations by introducing the characteristic length and time scales, L and L/U_0, and the swimming parameter $v_s = v_p/U_0$.

Let us first consider the time-independent cellular flow. To monitor the distribution of the particles in a finite domain we apply periodic boundary conditions on the unit square. For spherical particles where $\alpha = 0$, from Eq. (4) and given the incompressibility of the flow, the trace of the Jacobian is zero, and according to Liouville's theorem there can be no contraction in phase space volume. However, for $\alpha \neq 0$ aggregation is possible and numerical simulations show that there is a nonuniform stationary distribution with the particle density increasing from the center of cells towards the separatrices. Figure 1 shows the asymptotic distribution for particles initially distributed uniformly in space with random initial orientations, for different values of α and v_s. Note that the nonuniformity of the distribution depends on the shape of the particles and is more pronounced for strongly elongated particles.

If we now consider the same trajectories on the infinite x-y plane, the particles can be divided into two categories: those which move between cells and participate in large scale transport and those which remain trapped within a single cell. In the absence of swimming all trajectories are bounded. When swimming is introduced, a chaotic region forms around the separatrices of the flow field in which particles can cross into different cells and follow unbounded trajectories. This region is separated from trapped particles which move on quasiperiodic orbits within a single cell by an invariant surface. Increasing the swimming velocity eventually destroys this transport barrier and all particles escape. The minimum velocity corresponding to the breakup of the last bounded orbit depends on the aspect ratio α, as shown in Fig. 2. In the limit $\alpha \to 1$ the minimum velocity required for escape of all particles vanishes. Thus, for $\alpha = 1$ swimming is a singular perturbation as arbitrarily weak swimming leads to accumulation of particles in a very thin chaotic region around the separatrix lines, in contrast to spatially uniform distribution of passive tracers. As $v_s \to 0$ the width of the chaotic region shrinks to zero resulting in a singular density.

We find qualitatively similar behavior in the time-periodic cellular flow. Here the region occupied by unbounded chaotic trajectories remains finite in the $v_s \to 0$ limit and coincides with the chaotic region of the passive particles. In the case $\alpha = 1$ all particles escape the ordered elliptic region and participate in large scale transport; thus, the chaotic mixing region is an attractor for the dynamics of swimming particles. Output from numerical simulations show this in Fig. 3.

For $\alpha < 1$ a threshold velocity exists for the preservation of transport barriers as in the time-independent case. Increasing the amplitude B reduces the size of the elliptic regions and therefore reduces this swimming velocity threshold (see Fig. 2). Varying the frequency ω does not qualitatively alter the structure of the flow and has no significant effect on the particle distribution.

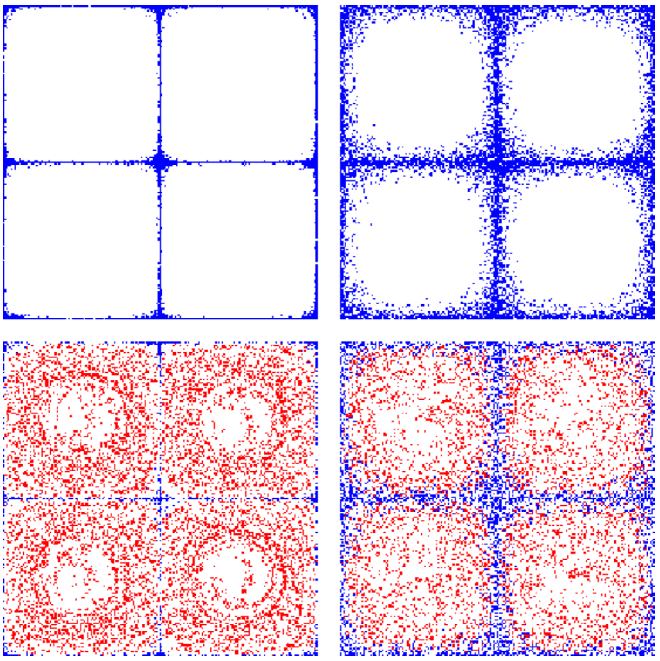

FIG. 1 (color online). Nonuniform steady state particle distribution. Top left: $\alpha = 1$, $v_s = 0.016$; top right: $\alpha = 1$, $v_s = 0.095$; bottom left: $\alpha = 0.9$, $v_s = 0.016$; bottom right: $\alpha = 0.7$, $v_s = 0.095$. Dark gray (blue) indicates particles which move between cells; light gray (red) are trapped particles.

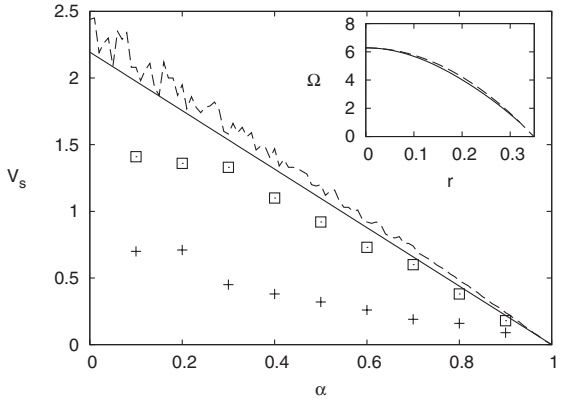

FIG. 2. Minimum velocity versus aspect ratio for nonexistence of transport barriers. The broken line indicates numerical results for the cellular flow; the solid line is a plot of the analytical result of Eq. (10). Data points show velocity threshold for the time-dependent case for $B = 0.12$ (+) and $B = 0.06$ (□). Inset: Angular velocity versus average radius for the cellular flow (solid line) and parabolic fit (broken line).

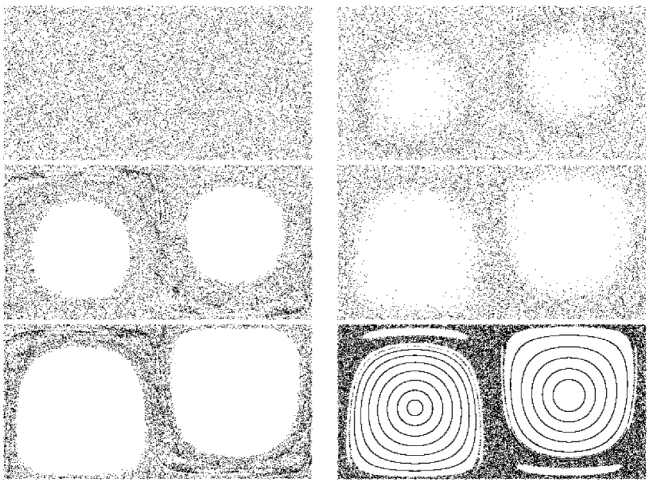

FIG. 3. Particles in time-dependent flow ($B = 0.12$, $\omega = 6.28$). Left: $V_s = 0.05$, $\alpha = 1$, snapshots taken at $\tau = 0, 12, 24$. Right: $V_s = 0.05$, $\alpha = 1$, $D_r = 0.5$, snapshots taken at $\tau = 50, 200$. Bottom right: Poincaré section for nonswimming particles in the same flow.

To study the impact of rotational diffusion we introduce an additive Gaussian noise term $\xi(t)$ to the first equation of (4), which satisfies $\langle \xi(t)\xi(t')\rangle = 2D_r\delta(t - t')$ where D_r is a diffusivity constant. Results are included in Fig. 3. The noise has the effect of slowing down the emptying of the central core and increasing slightly the width of the chaotic region. Our investigations indicate for $D_r \lesssim U_0/L$ emptying of elliptic regions occurs. As the intensity of the noise is increased further the effects are gradually lost and eventually particle distribution remains constant.

The behavior observed in the numerical simulations can be explained by an analysis of the dynamics of self-propelled particles within an elliptic island, that we approximate by a circularly symmetric vortex with angular velocity $\Omega(r)$. Neglecting for the moment the particle's motility, the equations of motion can be expressed in polar coordinates as

$$\dot{\beta} = \Omega(r), \qquad \dot{\theta} = \Omega(r) + \frac{r}{2}\frac{d\Omega}{dr}[1 + \alpha\cos(2\beta - 2\theta)], \tag{5}$$

where β is the angle of the position vector and θ is the orientation angle of the particle. This leaves a system of two coupled oscillators characterized by the phase difference $\phi = \theta - \beta$, that is the orientation of the particle with respect to the radial direction

$$\dot{\phi} = \frac{r}{2}\frac{d\Omega}{dr}[1 + \alpha\cos(2\phi)]. \tag{6}$$

For $\alpha < 1$ the phase difference changes monotonically. A bifurcation occurs at $\alpha = 1$ and semistable fixed points exist along the line $\phi^* = \pm\pi/2$. The system is therefore driven to synchrony, with the particles oriented tangentially to the streamlines. Note that when the swimming velocity is zero the two orientations $\pm\pi/2$ are equivalent. This behavior occurs for any nonconstant $\Omega(r)$.

If we now introduce a swimming velocity into Eq. (5) and express it in terms of the phase difference ϕ, we have

$$\begin{aligned} \dot{r} &= v_p\cos(\phi), \\ \dot{\phi} &= -\frac{v_p}{r}\sin(\phi) + \frac{r}{2}\frac{d\Omega}{dr}[1 + \alpha\cos(2\phi)]. \end{aligned} \tag{7}$$

For the special case of a solid body rotation the second term of the second line of Eq. (7) is zero. This results in the particle rotating with the same angular velocity as the flow. In a corotating frame of reference the particle will swim in a straight line and, as its dynamics are independent of α, no aggregation of particles is possible.

For nonconstant angular velocity the simplest functional form (resulting from a Taylor expansion around the center) is $\Omega(r) = \Omega_0[1 - (r/R_0)^2]$. This quadratic form agrees well with the angular velocity of the rotation along the streamlines of the cellular flow (see the inset in Fig. 2). However, the qualitative behavior is not sensitive to the particular form of $\Omega(r)$, and other monotonically decreasing functions yield similar results. We assume that r is restricted to $0 < r < R_0$, where R_0 represents the radius of a finite nonchaotic region in a flow.

Nondimensionalizing the equations with time scale $1/\Omega_0$, length scale R_0, and introducing the nondimensional swimming velocity $v_s = v_p/(R_0\Omega_0)$, we obtain

$$\begin{aligned} \dot{r} &= v_s\cos(\phi), \\ \dot{\phi} &= -\frac{v_s}{r}\sin(\phi) - r^2[1 + \alpha\cos(2\phi)]. \end{aligned} \tag{8}$$

In the central region, $r \ll v_s^{1/3}$, the last term in the second equation is small and the remaining system describes a particle moving freely with constant velocity and orientation in the corotating frame. Any such particle eventually leaves the central region, after which the reorientation due to the flow becomes important. Here the structure of the phase space can be characterized by the location of the ϕ nullclines

$$\phi(r) = \arcsin\left[\frac{v_s}{4\alpha r^3} - \sqrt{\left(\frac{v_s}{4\alpha r^3}\right)^2 + \frac{1+\alpha}{2\alpha}}\right]. \tag{9}$$

These nullclines, which separate regions of clockwise and counterclockwise rotations in the phase space, are composed of two symmetric branches along the $\phi = -\pi/2$ axis. Phase diagrams are shown in Fig. 4.

For $\alpha = 1$ the system (8) has no fixed points, the half-stable fixed point of the nonswimming particles at $+\pi/2$ has disappeared, while the one at $-\pi/2$ has split into two branches of quasisteady states. Thus the only stable orientation is now swimming against the direction of the flow. Equation (9) has solutions for all values of r; therefore, the nullclines extend to infinity and at no point is a particle able to complete a full rotation relative to the flow. When $r > v_s^{1/3}$, the trajectories approach the stable right branch of the

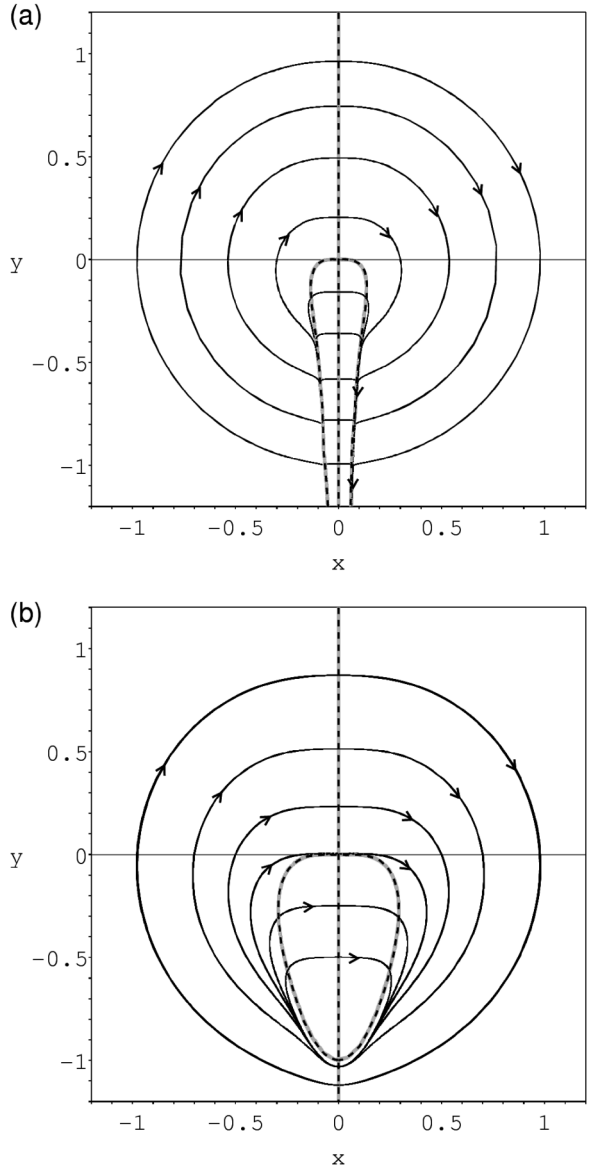

FIG. 4. Phase plane diagrams for (a) $\alpha = 1.0$, $v_s = 0.01$ and (b) $\alpha = 0.9$, $v_s = 0.1$. The nullclines are shown by dashed lines, axes represent spatial coordinates in a corotating frame.

ϕ nullcline where $\dot{r}$ is positive and move away from the center indefinitely.

When $\alpha < 1$ there is an intersection between the ϕ nullclines and r nullcline which is along $\phi = -\pi/2$, creating a fixed point with purely imaginary eigenvalues at $r^* = [v_s/(1-\alpha)]^{1/3}$, $\phi^* = -\pi/2$. At this point the two branches of solutions of Eq. (9) coalesce and no real solutions exist in the region $r > r^*$. All trajectories are closed periodic orbits that rotate around the fixed point alternating between swimming towards or away from the vortex center. The largest distance from the center on a given trajectory is reached at $\phi = -\pi/2$, and satisfies the condition $r_{\max} > r^*$.

Since we assumed that the vortex flow within the unit circle represents a finite elliptic island surrounded by a chaotic flow region, we obtain a condition for the nonexistence of closed orbits within the unit circle, as $r^* > 1$, that in dimensional form is equivalent to

$$v_p > R_0\Omega_0(1-\alpha). \tag{10}$$

This explains the linear dependence of the threshold swimming velocity on the aspect ratio seen in the numerical simulations. Substituting the angular velocity in the elliptic points of the cellular flow, $\Omega_0 = 2\pi U_0/L$, and the maximum time-averaged radius of the cellular flow trajectories estimated numerically as $R_0 \approx 0.35L$, we obtain a good agreement with the numerical threshold velocity needed for the breakup of the last transport barrier (see Fig. 2).

Thus we have shown that for a finite circular vortex region there is a minimum swimming velocity such that all particles leave the vortex. When the vortex is surrounded by a chaotic region the particles may also enter the regular flow region from outside; however, since in hyperbolic regions of the flow elongated particles are mostly oriented along the Lyapunov vectors (i.e., stretching direction), this results in a smaller particle density inside the vortex. In the particular case $\alpha = 1$, particles in the chaotic region are oriented exactly in the direction of the Lyapunov vectors, that is tangent to the elliptic region of the flow at the boundaries; thus, particles cannot enter from outside and the density inside the vortex goes to zero.

The accumulation of swimming microorganisms in chaotic regions of a fluid flow can be advantageous for fast dispersion and for avoiding closed regions that could become depleted of nutrients. Thus swimming can be an efficient evolutionary strategy even without the complex biological mechanisms necessary for oriented swimming in response to external fields. It would be interesting to test the predictions of this model in an experimental setting and could provide for a mechanism where particles of different shape or motility are separated.

[1] T. J. Pedley and J. O. Kessler, Annu. Rev. Fluid Mech. **24**, 313 (1992).
[2] C. Dombrowski, L. Cisneros, S. Chatkaew, R. E. Goldstein, and J. O. Kessler, Phys. Rev. Lett. **93** 098103 (2004).
[3] T. Vicsek, A. Czirók, E. Ben-Jacob, I. Cohen, and O. Shochet, Phys. Rev. Lett. **75**, 1226 (1995).
[4] J. P. Hernandez-Ortiz, C. G. Stoltz, and M. D. Graham, Phys. Rev. Lett. **95**, 204501 (2005).
[5] G. B. Jeffery, Proc. R. Soc. A **102**, 161 (1922).
[6] J. M. Ottino, *The Kinematics of Mixing: Stretching, Chaos, and Transport* (Cambridge University Press, Cambridge, 1989), p. 375.
[7] T. H. Solomon and I. Mezić, Nature (London) **425**, 376 (2003).
[8] T. H. Solomon and J. P. Gollub, Phys. Rev. A **38**, 6280 (1988).